Measurement of magnetic dipole moments of $^{129}Xe^m$ and $^{131}Xe^m$ by spin exchange with optically pumped Rb

M. Kitano,* M. Bourzutschky, F. P. Calaprice, J. Clayhold, W. Happer, and M. Musolf
Department of Physics, Princeton University, Princeton, New Jersey 08544
(Received 9 April 1986)

The magnetic moments of xenon atoms ($^{129}Xe^m$ and $^{131}Xe^m$) have been measured with a high precision nuclear-magnetic-resonance method. The nuclei of gaseous xenon were polarized by spin exchange with optically pumped rubidium and the polarization was measured by gamma-ray anisotropy. The static magnetic field for the nuclear magnetic resonance experiment was stabilized and calibrated by optical pumping magnetometers. The measured magnetic moments are $|\mu(129m)| = 0.891\,223(4)\,\mu_N$ and $|\mu(131m)| = 0.994\,048(6)\,\mu_N$.

I. INTRODUCTION

In a previous paper,[1] a new experimental method was established to produce highly polarized nuclei of radioactive noble gases. The method utilizes spin exchange and gamma-ray anisotropy detection. The nuclei of xenon gases can be polarized by spin exchange with alkali atoms (e.g., Rb) which have been spin polarized by optical pumping. The spin exchange can be represented schematically as follows:

$$\mathrm{Rb}(\uparrow)+\mathrm{Xe}(\downarrow)\rightarrow\mathrm{Rb}(\downarrow)+\mathrm{Xe}(\uparrow)\ . \tag{1}$$

The polarization of helium atoms by spin exchange with optically polarized alkali was first observed by Bouchiat, Carver, and Varnum.[2] Grover[3] showed that, for heavier noble gas atoms like Kr and Xe, the reaction is strongly enhanced. The reason for the enhancement is explained by the formation of alkali-noble-gas van der Waals molecules.[4,5] A third body, a N_2 molecule in our experiment, is needed to allow the formation of such a molecule.

With this method, radioactive xenon nuclei, $^{131}Xe^m$, $^{133}Xe^m$, and ^{133}Xe, were polarized. The maximum polarization achieved was characterized by a dimensionless spin temperature parameter $\beta=0.38$. For comparison we note that the corresponding polarization could be achieved by cooling the nuclei down to ~ 10 mK under a magnetic field of ~ 1000 kG.

The polarization in radioactive nuclei can be detected by observing the anisotropy of the gamma ray radiation. The angular distribution of gamma rays emitted from oriented nuclei in a state characterized by the spin density matrix $\rho=\sum_{k=0}\rho_k T_0^{(k)}$ can be expressed as a series of Legendre polynomials $P_k(\cos\theta)$,

$$W(\theta)=1+\rho_2 F_2 P_2(\cos\theta)+\rho_4 F_4 P_4(\cos\theta)+\cdots\ , \tag{2}$$

where $T_0^{(k)}$ is the longitudinal tensor operator of kth order and θ is the angle between the orientation axis and the direction of the gamma ray. The coefficient F_k depends on the initial and the final nuclear states and the multipolarity of the radiation.[6]

As an application of our method, the magnetic dipole moments of the above-mentioned isotopes were measured. Their accuracy of ~ 300 parts per million (ppm) is satisfactory in view of comparison with theories. In principle, however, an accuracy of ~ 0.1 ppm could be possible, because the long nuclear-spin relaxation time would result in very narrow nuclear magnetic resonance (NMR) linewidths ($\sim$mHz). One of our aims of this work is to improve the accuracy. Special attention has been paid to produce a stable and accurately calibrated magnetic field.

Another aim is to measure the magnetic of $^{129}Xe^m$. In our previous experiments, this isotope was not found in a reactor-produced sample of ^{133}Xe which contained traces of $^{131}Xe^m$ and $^{133}Xe^m$. In this work, $^{129}Xe^m$ has been produced from tellurium bombarded with alpha particles.

Conventional methods which have been used to measure magnetic moments of long-lived xenon nuclei are divided into two categories: (1) low temperature methods [nuclear orientation (NO) (Ref. 7) and nuclear magnetic resonance on oriented nuclei (NMR/ON) (Ref. 8)]; and (2) laser hyperfine spectroscopy of atomic excited states.[9] In both methods, xenon nuclei are exposed to a hyperfine field, which cannot be estimated with high accuracy. On the other hand, for the case of free-atom NMR's, the field at the nucleus is determined unambiguously by external field measurements (except for a diamagnetism correction). Accurate magnetic moments measured by this direct method can be helpful to determine the above-mentioned crystalline or atomic hyperfine fields.

In the course of these experiments we also develop methods for narrow resonance NMR's which can be applied to other experiments, such as the search for nuclear electric dipole moments.[10]

II. PRODUCTION OF Xe ISOTOPES

Natural tellurium was bombarded with 40 MeV α particles from the Princeton Cyclotron to produce xenon isotopes. We made a target by filling a shallow dip (8 mm diameter, 1 mm depth) on an aluminum heat sink, ($10\times 20\times 4$ mm) with molten tellurium. After bombardment for three hours at 0.5 μA, the target was put into a glass vacuum vessel to which a Pyrex glass cell with 1 cm diameter had been connected through a breakable seal

with a constriction for sealoff. A small amount of rubidium metal and 0.5 Torr of natural xenon had been preloaded into the cell. After the system was evacuated to a pressure of 10^{-6} Torr or less, it was isolated from the vacuum pump. To liberate xenon atoms from the tellurium pellet, the target was heated up to the melting point (550°C). After a potassium getter was activated to remove impurities, the breakable seal was opened. About half of the radioactive xenon atoms, along with the natural xenon, was condensed into the Pyrex cell by cooling with liquid N_2. The cell was sealed off from the vacuum system with a torch after 50 Torr of N_2 gas was introduced. The analysis of the gamma ray spectra showed that the following xenon isotopes were produced: ^{125}Xe ($\frac{1}{2}^+$, 17 h); ^{127}Xe ($\frac{1}{2}^+$, 30 d); ^{129}Xe^m ($\frac{11}{2}^-$, 8 d); ^{131}Xe^m ($\frac{11}{2}^-$, 11 d); ^{133}Xe^m ($\frac{11}{2}^-$, 2 d); and ^{133}Xe ($\frac{3}{2}^+$, 5 d). In this experiment we used the 164 keV gamma ray of ^{131}Xe^m and the 196.6 keV gamma ray of ^{129}Xe^m.

III. STABILIZATION AND CALIBRATION OF THE MAGNETIC FIELD

To measure magnetic moments very precisely, a stable and homogeneous magnetic field is required along with sufficiently accurate field calibration. In our previous experiments,[1] three pairs of Helmholz coils were used and linewidths narrower than 0.5 Hz could not be obtained owing to external magnetic field fluctuations. For this experiment, a solenoid magnet (30 cm diam and 100 cm length) was prepared with triple mu metal shielding to exclude external fields. Although with this magnet we observed 0.02–0.06 Hz linewidths,[11] the reproducibility was found to be poor. This suggests that the long-term stability of the field is about 100 μG. Apparently, the field was still affected by nearby apparatus and also by the thermal expansion of the coil itself, and additional improvements were required.

A. Stabilization

For further improvement of the field stability, an active field-locking system was developed using optical pumping magnetometry. Figure 1 shows the block diagram of the locking system. The principle of operation is described in detail in Ref. 12. We chose ^{133}Cs as an active medium instead of ^{87}Rb which was used by Farr and Otten[13] because the rf field for magnetometry might destroy the Rb polarization in the xenon NMR cell. [The gyromagnetic ratio of $\gamma(^{133}\text{Cs}) \approx 350$ kHz/G is different from either $\gamma(^{87}\text{Rb}) \approx 700$ kHz/G or $\gamma(^{85}\text{Rb}) \approx 467$ kHz/G.]

The probe box was designed so that the Cs cell is located close (2 cm) to the Xe cell to minimize the field differences due to inhomogeneity in the magnetic field. The optimum temperature (≈ 60°C) for the Cs cell is maintained by a cool air flow in the gap between the probe box and the oven for the Xe cell which is heated to 150°C by flowing hot air.

The light of a Cs lamp in a separate enclosure is guided by an optical fiber bundle (11 mm diam) into the probe box, passes through a circular polarizer and the Cs cell, and is detected by a Si photo detector. The photo signal is amplified by a current amplifier and is fed to a lock-in amplifier.

A rf magnetic field is generated by a small pair of coils around the cell and a frequency synthesizer (HP3325A/001, aging rate of frequency: $\pm 5 \times 10^{-8}$ per week, $\pm 1 \times 10^{-7}$ per month). The rf current from the synthesizer is frequency-modulated by the lock-in reference signal (160 Hz) in order to detect a differentiated resonance signal by the lock-in amplifier.

Figure 2 shows a typical resonance signal which was obtained by sweeping the rf frequency across the resonances. The static field was maintained at ≈ 8 G by feeding a constant current to the solenoid. Each resonance

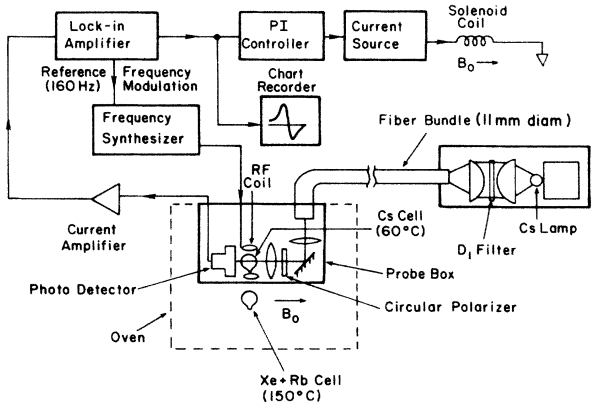

FIG. 1. Block diagram of field-locking system with Cs magnetometer.

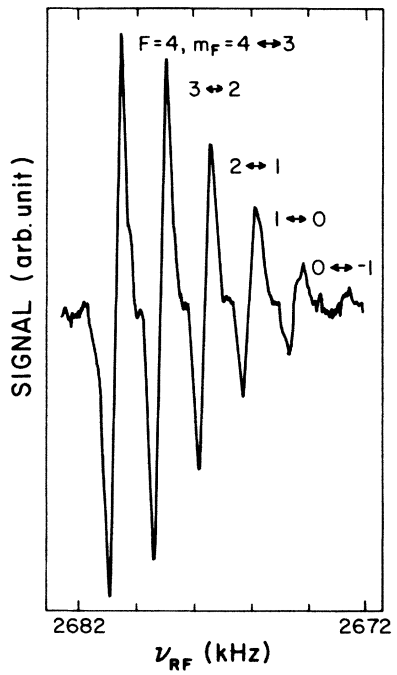

FIG. 2. Resonance signal using Cs magnetometer.

can be labeled by the related levels (F,m_F) and $(F,m_F'=m_F\pm1)$ between which the transition takes place. Usually, the resonance $(F=4,m_F=-3\leftrightarrow-4)$ was used which gives the largest signal for σ_+ light. [For σ_- light $(F=4,m_F=3\leftrightarrow4)$ is the largest.]

The transition frequency $\nu(B_0)$ is related to the static magnetic field B_0 through the Breit-Rabi formula.[12,13] The atomic constants in the formula are known to high accuracy.[12,14,15] The inaccuracy in the formula is dominated by the uncertainty of μ_B/h, which is a few ppm. However, the accuracy is improved to 0.1 ppm, the error in the g_J values,[14,12] when the field is measured in units of μ_B/h. Even when it is measured in units of μ_N, the inaccuracy is less than 1 ppm, because the ratio $\mu_N/\mu_B=m_p/m_e$ is known with the accuracy of 3.8×10^{-7}.

It should be noted in Fig. 2 that around the resonance center the output ϵ of the lock-in amplifier is proportional to the mistuning; namely,

$$\epsilon=\beta[\nu_{RF}-\nu(B_0)]\ , \tag{3}$$

where β is a constant and ν_{RF} is the frequency of the rf field. By feeding the error signal ϵ to the current source of the solenoid coil, the magnetic field can be controlled so as to satisfy the relation $\epsilon=0$ or $\nu(B_0)=\nu_{RF}$. Thus the field can be locked to the value of $B_0=\nu^{-1}(\nu_{RF})$. A proportional-integral (PI) controller allows us to adjust the loop gain and the time constant to optimize the performance.

Throughout this experiment, we used

$$\nu_{RF}=3\,003\,600\ \text{Hz}\ , \tag{4}$$

which corresponds to the field value

$$B_0^{Cs}=8.565\,610(10)\ \text{G}\ . \tag{5}$$

The error in B_0^{Cs} (10 μG, 1.2 ppm) was estimated from the residual error signal and the system noise level. The uncertainty due to the atomic constants estimated above has been neglected. We note that the absolute frequency of the synthesizer is not so important because we effectively measure a ratio of resonance frequencies to determine the xenon magnetic moments. So we quoted no uncertainty for ν_{RF} in Eq. (4).

B. Calibration

Since the Xe cell is 2 cm away from the Cs cell, the field B_0^{Xe} at the Xe cell has to be measured under the field-locked condition by another independent magnetometer. The ^{87}Rb and ^{85}Rb atoms in the Xe cell were used for the magnetometry. The temperature of the oven was lowered down to 80 °C so that weak pumping light (<1 mW) can penetrate through the cell.

A single-mode diode laser (GaAlAs,RCA RS-28T) tuned to the rubidium D_1 line was used as the light source for ease of beam handling. The transmitted light is detected by a Si photo cell which is located between the oven and the gamma ray detector. (See Fig. 3.)

A frequency-modulated rf field is generated by a pair of Helmholz coils and a frequency synthesizer (HP3325A). The master oscillator of the synthesizer is frequency locked to the reference signal of the other synthesizer for field locking. This assures high accuracy in the ratio of two frequencies. We can nullify the output of the lock-in amplifier by adjusting the rf frequency to find a resonance frequency of Rb.

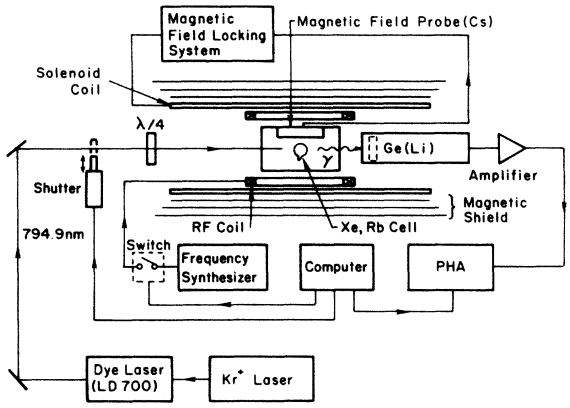

FIG. 3. Experimental setup for NMR studies.

A disadvantage of using the diode laser is that, due to its narrow light spectrum, a light shift of the Zeeman frequency occurs.[16] The offset in the magnetic field caused by the shift was found to be ≈400 μG in the case of ^{87}Rb. Since the offset changes sign according to the polarization of the pumping light, the effect can be canceled by taking a pair of data: one by σ_+ and the other by σ_- light.

We measured the field value as

$$B_0^{Xe}=8.565\,318(10)\ \text{G}\ . \tag{6}$$

We estimate the fluctuation of the difference $\Delta B=B_0^{Cs}-B_0^{Xe}$ (≈292 μG), because it may deteriorate the stability of B_0^{Xe} as compared to that of B_0^{Cs}. The difference ΔB, which is due to the finite size of the solenoid, could be effected by the current change for the field compensation. The maximum current change observed was ~400 ppm and would affect ΔB by 0.12 μG. The variation in ΔB owing to external field inhomogeneity is expected to be less than 1 μG. Thus the stability of B_0^{Xe} should be comparable to that of B_0^{Cs}. Actually we confirmed the stability of measuring B_0^{Xe} repeatedly.

IV. NMR METHOD

In the previous work, the accuracy of the magnetic moment was limited by the uncertainty in the effective field experienced by xenon atoms due to collisions with polarized Rb atoms.[3] This field, which was estimated to be ≈3 mG at a cell temperature 150 °C, depends on the cell temperature and on the pumping laser power. This effective field cannot be compensated by the field-locking system. The contribution could be canceled out to some extent by measuring the resonance frequencies both for σ_+ and σ_- pumping light and taking their average.[11] But it is not easy to cancel it completely because it is strongly temperature dependent (≈100 μG per °C).

A new NMR method which we use here spares us the

trouble. The point is to quench the Rb polarization during the NMR measurement by blocking the pumping light. The experimental procedure consists of two phases. In the polarizing phase (≈ 2 min), the xenon nuclei are polarized to the saturation level by spin exchange collisions with the laser polarized rubidium atoms. In the NMR phase (30 sec), the rf field of a frequency ω_i is applied and a gate for gamma-ray counting instruments is open, while the laser beam is blocked. During this phase, the xenon nuclei are free from the effective field because the polarization in the rubidium atoms dies quickly (~ 1 msec) after the laser beam has been blocked. (A small effective field caused by repolarization of Rb due to natural xenon is estimated to be less than 3 μG and is negligible in our case.) At the end of this phase, the gamma-ray count C_i is recorded. This cycle is repeated while the rf frequency ω_i is changed over a resonance frequency. By plotting the data (ω_i, C_i), we can see a resonance signal.

V. EXPERIMENT

The experimental setup for Xe NMR's is shown in Fig. 3. A krypton laser (Coherent CR3000K) is used to pump a dye laser (Coherent 699, standing wave mode, dye: LD700), which produces 1 W of light resonant to the rubidium D_1 line (794.7 nm) with a bandwidth of ≈ 30 GHz. The light is circularly polarized by a $\lambda/4$ plate and illuminates the Xe cell in the oven. The magnetic field at the cell is stabilized and calibrated as described in Sec. III.

The gamma-ray energy spectrum is measured with a Ge(Li) detector (Princeton Gamma-Tech LGC26ACD, 54 mm diam, 22 mm drift depth), modified to eliminate magnetic materials near the detector, and a multichannel pulse height analyser (PHA). Magnetic resonance in the xenon nuclei is induced by the same set of coils and synthesizer which were used for the field calibration.

To realize the transient NMR method described in the preceding section, a computer (Apple II +) is used to control the following devices according to the following time sequence: a switch for the rf current, a shutter of the laser beam, and a gate for PHA.

A typical resonance pattern of $^{129}Xe^m$ is shown in Fig. 4. The non-Lorentzian line shape is expected from theoretical calculations. Generally speaking, a contribution of the $P_k(\cos\theta)$ term in Eq. (2) to the NMR signal produces a k-fold split resonance for cases $\omega_1/\gamma \gtrsim 1$, where ω_1 and γ are the amplitude of the rf field and the spin relaxation rate, respectively.[17] In our case, where the gamma-ray anisotropy is well represented by the $P_2(\cos\theta)$ term and the condition $\omega_1/\gamma \gtrsim 1$ is satisfied ($\omega_1 \approx 0.15$ sec^{-1}, $\gamma \approx 0.03$ sec^{-1}), we should see a line shape with a single dip. The line shape can be expressed as

$$B(\omega-\omega_0)=1-\tfrac{3}{4}\omega_1^2\frac{4(\omega-\omega_0)^2+\omega_1^2}{[(\omega-\omega_0)^2+\omega_1^2]^2}\ , \tag{7}$$

where ω and ω_0 are the rf frequency and the resonance frequency, respectively.

In 1952, Brossel and Bitter[18] studied this line shape for optical-double-resonance lines in Hg isotopes. A good geometrical interpretation of the line shape is given in Ref. 17.

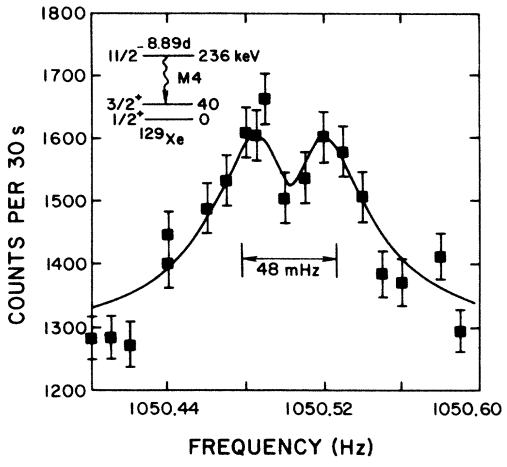

FIG. 4. Typical NMR resonance pattern for the $^{129}Xe^m$ nucleus. The solid line shows the best-fit curve of the form

$$y=a_1+a_2[4(x-a_3)^2+a_4^2]/[(x-a_3)^2+a_4^2]^2\ .$$

Error bars indicate only Poisson uncertainty. The fitted parameters are $a_1=1284(10)$, $a_2=0.136(12)$, $a_3=1050.5027(21)$, $a_4=0.0239(20)$.

A curve-fitting program was used to determine the centroids for the resonances of $^{129}Xe^m$ and $^{131}Xe^m$, which were found to be

$$\nu_{129m}=1050.5027(45)\ \text{Hz} \tag{8}$$

and

$$\nu_{131m}=1171.7046(73)\ \text{Hz}\ , \tag{9}$$

respectively. In determining the uncertainties, we have taken into account the fluctuation of the initial Xe polarization ($\sim 5\%$) in addition to the Poisson uncertainty.

Using the magnetic field value Eq. (6), we determine the magnetic moments listed in the third column of Table I. The values were corrected for diamagnetism with $1/(1-\sigma)=1.007\,092$ with no allowance for the uncertainty in σ.[15] The accuracy (4—7 ppm) has been improved substantially compared to our previous results. We also recalculated the moments of $^{133}Xe^m$ and ^{133}Xe based on the frequency ratios ν_{133m}/ν_{131m} and ν_{133}/ν_{131m} which were measured in Ref. 1. In the fourth column, the values obtained in our previous works[1,11] are listed, all of which are consistent with the new values. Especially, it should be stressed that, for $^{131}Xe^m$, in spite of the use of completely independent setups, μ_{old} and μ_{new} are in good agreement.

VI. DISCUSSION

In Table I, both of our values for ^{133}Xe differ from that of Ref. 9, which was obtained by laser hyperfine measurements, by $10^{-3}\ \mu_N$, or about 3 times the latter's uncertain-

TABLE I. Magnetic moments of Xe isotopes. The values are corrected for diamagnetism with $1/(1-\sigma)=1.007092$. See Ref. 15.

Isotope	J^π	$\lvert\mu_{new}\rvert$ (μ_N)	$\lvert\mu_{old}\rvert$ (μ_N)	$\mu_{previous}$ (μ_N)	$\mu_{Schmidt}$ (μ_N)
$^{129}Xe^m$	$\frac{11}{2}^-$	0.891 223(4)	0.891 51(34)[b]	−0.847(28)[d]	−1.91
$^{131}Xe^m$	$\frac{11}{2}^-$	0.994 048(6)	0.994 35(38)[c]	−0.80(10)[e]	−1.91
$^{133}Xe^m$	$\frac{11}{2}^-$	1.082 47(15)[a]	1.082 79(45)[c]	−0.87(12)[e]	−1.91
^{133}Xe	$\frac{3}{2}^+$	0.813 40(7)[a]	0.813 65(32)[c]	+0.8125(3)[f]	+1.15

[a]Based on the NMR frequency ratio to that of $^{131}Xe^m$ measured in Ref. 1.
[b]Spin exchange (Ref. 11).
[c]Spin exchange (Ref. 1).
[d]NMR/ON (Ref. 8).
[e]NO (Ref. 7).
[f]Hyperfine measurement by laser spectroscopy (Ref. 9).

ty. Their value was derived from the hyperfine constant ratios and the known moments of stable isotopes, so the discrepancy might be attributed to the hyperfine anomaly.

In Fig. 5, our data for the three $\frac{11}{2}^-$ isomers ($^{129}Xe^m$, $^{131}Xe^m$, $^{133}Xe^m$) are plotted together with previous data obtained by cryogenic methods.[7,8] Our data show almost perfect linear relationship between the magnetic moment and the mass number A. The slope is $-0.095\ \mu_N$ per neutron pair.

We note, in Fig. 5, that there are considerable disagreements with the previous measurements. In particular, the data for $^{131}Xe^m$ and $^{133}Xe^m$ by Silverans *et al.*[7] are smaller than ours by twice their uncertainty. It is reasonable to attribute these discrepancies to the misevaluation in their work of the hyperfine field of xenon nuclei at substitutional sites in the iron foil. In their nuclear orientation (NO) experiment, to determine the magnetic moment, they used an effective iron hyperfine field H which had been evaluated by Pattyn *et al.*[19] Pattyn *et al.* measured $|\mu_{3/2}(133)H|$ by NO. In order to determine H, they used a value of $\mu_{3/2}(133)=0.72(5)$ which was estimated from the well-known $\mu_{3/2}(131)$ (stable) and a theoretically predicted increase of 0.03 μ_N associated with the addition of a pair of neutrons. Now

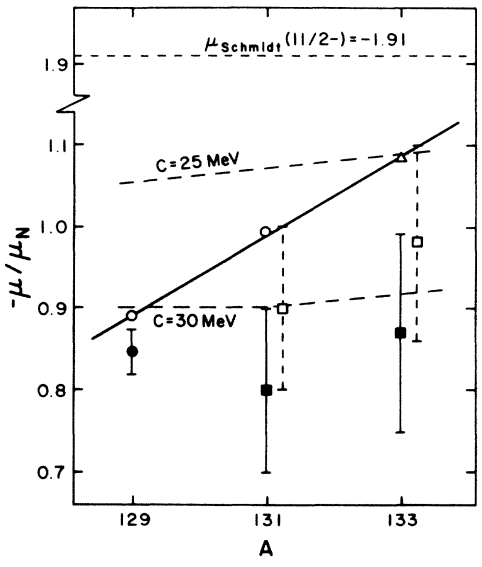

FIG. 5. Magnetic moments of $\frac{11}{2}^-$ isotopes. Our data are shown by open circles and a triangle. The closed circle and squares represent data from Refs. 8 and 7, respectively. Open squares show recalculated values of Ref. 7 based on our data for ^{133}Xe. The two dashed lines represent theoretical values taken from Ref. 7.

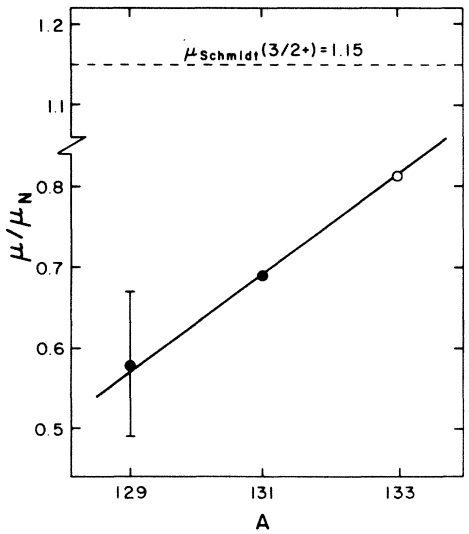

FIG. 6. Magnetic moments of $\frac{3}{2}^+$ isotopes. The open circle represents our value. The values for $A=129$ and 131 (closed circles) are taken from Ref. 15.

we have a more reliable and more accurate value of $\mu_{3/2}(133)=0.813\ldots$ and can recalculate H and the magnetic moments of Silverans *et al.* as $\mu_{11/2}(131m) = -0.90(10)$ and $\mu_{11/2}(133m) = -0.98(12)$. We plotted the recalculated values in Fig. 5 (open squares). These are now consistent with our values.

It is worthwhile to notice that the magnetic moment increases from ^{131}Xe($\frac{3}{2}$) to ^{133}Xe($\frac{3}{2}$) by 0.122 μ_N, which is four times as large as 0.03 μ_N given above.[19] This increase is very close to that between accepted values, $\mu_{3/2}(129)=-0.58(9)$ and $\mu_{3/2}(131)=-0.691\,861(4)$.[15] Namely, also for the $\frac{3}{2}^+$ states, there is a linear relationship between the magnetic moments and the mass number A as plotted in Fig. 6, although it is not conclusive owing to the large uncertainty in $\mu_{3/2}(129)$.

The dashed lines in Fig. 5 represent theoretical values calculated by Silverans *et al.*[7] They used the spin polarization procedure based on wave functions from the pairing-plus-quadrupole model.[20] The upper (lower) line is for the pairing strength parameter $C=25$ (30) MeV. Silverans *et al.* concluded that the theoretical values for $C=30$ MeV agree with their experimental results. But our new data suggest that the use of a common value for different isomers is not appropriate. Instead we can choose $C=30$ MeV for ^{129}Xe^m, 27.5 MeV for ^{131}Xe^m, and 25 MeV for ^{133}Xe^m to see good agreement. A similar discussion on the choice of C for Hg isomers is found in Ref. 21.

Recently, Arias *et al.*[22] calculated magnetic moments for Xe $\frac{11}{2}^-$ states by using the interacting boson-fermion model. Their values (~ -1.3 μ_N for all isomers) are significantly larger in absolute value than the experimental data. They suggested the inclusion of higher lying single particle orbitals would improve the quantitative agreement.

ACKNOWLEDGMENT

We wish to thank Zhen Wu for many helpful discussions. This work was supported by the National Science Foundation and the U.S. Army Research Office under Grant No. DAAG-29-83-K-0072.

*Permanent address: Radio Atmospheric Science Center, Kyoto University, Uji, Kyoto 611, Japan.

[1]F. Calaprice, W. Happer, D. Schreiber, M. Lowry, E. Miron, and X. Zeng, Phys. Rev. Lett. **54**, 174 (1985).

[2]M. A. Bouchiat, T. R. Carver, and C. M. Varnum, Phys. Rev. Lett. **5**, 373 (1960).

[3]B. C. Grover, Phys. Rev. Lett. **40**, 391 (1978).

[4]C. H. Volk, T. M. Kwon, and J. G. Mark, Phys. Rev. A **21**, 1549 (1980).

[5]W. Happer, E. Miron, S. Schaefer, D. Schreiber, W. A. van Wijngaarden, and X. Zeng, Phys. Rev. A **29**, 3092 (1984).

[6]T. Yamazaki, Nucl. Data Sect. A **3**, 1 (1967).

[7]R. Silverans, R. Coussement, H. Pattyn, E. Schoeters, and L. Vanneste, Z. Phys. **267**, 145 (1974).

[8]E. Schoeters, R. Coussement, R. Geerts, J. Odeurs, H. Pattyn, R. Silverans, and L. Vanneste, Phys. Rev. Lett. **37**, 302 (1976).

[9]F. Schneider, W. Makat, E. Mathias, R. Went, and P. West, in *Lasers in Nuclear Physics,* edited by C. E. Bemis and H. K. Carter, Nuclear Science Research Conference Series Vol. 3 (Harwood Academic, Chur, 1982).

[10]T. G. Vold, F. J. Raab, B. Heckel, and E. N. Fortson, Phys. Rev. Lett. **52**, 2229 (1984).

[11]F. Calaprice, J. Clayhold, W. Happer, M. Kitano, and M. Musolf, The Princeton University Cyclotron Annual Report for 1984 (unpublished), p. 13.

[12]W. Farr and E. W. Otten, Appl. Phys. **3**, 367 (1974).

[13]N. F. Ramsay, *Molecular Beams* (Oxford University Press, Oxford, 1955).

[14]E. Arimondo, M. Inguscio, and P. Violino, Rev. Mod. Phys. **49**, 31 (1977).

[15]*Tables of Isotopes,* 7th ed., edited by C. M. Lederer and V. S. Shirley (Wiley, New York, 1978).

[16]W. Happer and B. S. Mathur, Phys. Rev. **163**, 12 (1967).

[17]E. Matthias, B. Olsen, D. A. Shirley, and J. E. Templeton, Phys. Rev. A **4**, 1626 (1971).

[18]J. Brossel and F. Bitter, Phys. Rev. **86**, 308 (1952).

[19]H. Pattyn, R. Coussement, G. Dumont, E. Schoeters, R. E. Silverans, and L. Vanneste, Phys. Lett. **45A**, 131 (1973).

[20]L. S. Kisslinger and R. A. Sorensen, Rev. Mod. Phys. **35**, 853 (1963); N. Freed and L. S. Kisslinger, Nucl. Phys. **25**, 611 (1961); H. Noya, A. Arima, and H. Horie, Prog. Theor. Phys. Suppl. **8**, 33 (1958); A. Arima and H. Hiroe, Prog. Theor. Phys. **12**, 623 (1954).

[21]R. J. Reiman and M. N. McDermott, Phys. Rev. C **7**, 2065 (1973).

[22]J. M. Arias, C. E. Alonso, and R. Bijker, Yale University report, 1985.